Quantitative assessment of ventilation-perfusion relationships with gallium-68 positron emission tomography/computed tomography imaging in lung cancer patients

Zhuorui Li [a], Pierre-Yves Le Roux [b], Jason Callahan [c], Nicholas Hardcastle [d,e], Michael S. Hofman [c,e], Shankar Siva [e,f], Tokihiro Yamamoto [g,*]

[a] Department of Biomedical Engineering, University of California Davis, Davis, CA, USA
[b] Department of Nuclear Medicine, Brest University Hospital, EA3878 (GETBO), Brest, France
[c] Molecular Imaging and Therapeutic Nuclear Medicine, Peter MacCallum Cancer Centre, Melbourne, Australia
[d] Department of Physical Sciences, Peter MacCallum Cancer Centre, Melbourne, Australia
[e] Sir Peter MacCallum Department of Oncology, The University of Melbourne, Parkville, Australia
[f] Department of Radiation Oncology, Peter MacCallum Cancer Centre, Melbourne, Australia
[g] Department of Radiation Oncology, University of California Davis School of Medicine, Sacramento, CA, USA

ARTICLE INFO

ABSTRACT

Pulmonary functional imaging has demonstrated potential to improve thoracic radiotherapy. The purpose of this study was twofold: 1) to quantify ventilation/perfusion relationships in lung cancer patients using a new functional imaging approach, gallium-68 (^{68}Ga)-positron emission tomography/computed tomography (PET/CT); and 2) to compare ventilation/perfusion matching with diffusing capacity of the lung for carbon monoxide (D_{LCO}). Voxel-wise correlations between ventilation and perfusion varied widely among 19 patients (range: 0.26–0.88). ^{68}Ga-PET/CT-measured percent gas exchanging lung volume was moderately correlated with D_{LCO} ($\leq$0.59). Our findings suggested that ^{68}Ga-PET/CT ventilation/perfusion imaging provided complementary information and a reasonable surrogate for gas exchange in lung cancer patients.

1. Introduction

Pulmonary functional imaging has the potential to improve thoracic radiotherapy (especially for lung cancer) and has been studied extensively [1]. Image-guided functional avoidance radiotherapy, an emerging strategy to preferentially avoid irradiating functionally normal lung regions, may reduce pulmonary toxicity (*e.g.*, radiation pneumonitis) compared with standard radiotherapy [1,2] and has been currently assessed in several clinical trials. Previous work on pulmonary functional imaging in radiotherapy has been largely based on ventilation or perfusion alone [1]. However, gas exchange is the primary function of the lungs. Local ventilation/perfusion (V/Q) matching is the most important mechanism determining gas exchange efficiency [3]. Although ventilation and perfusion are well matched in the normal lung, V/Q mismatch occurs under pathological conditions [3]. Data on V/Q matching in lung cancer is scarce and there have only been a few studies using single-photon emission computed tomography (SPECT) [4–6],

which is limited by poor spatial resolution and regarded as nonquantitative (due to lack of corrections for photon attenuation and scattering). Moreover, technetium-99 m (^{99m}Tc)-diethylenetriamine pentaacetate (DTPA) aerosols, one of the most commonly used radiotracers for ventilation imaging with scintigraphy or SPECT, suffer from clumping in central airways, leading to artifacts with spurious image values, particularly in patients with chronic obstructive pulmonary disease (COPD) [6,7].

A new lung functional imaging approach, gallium-68 (^{68}Ga)-Galligas/^{68}Ga-macroaggregated albumin (MAA) positron emission tomography/computed tomography (PET/CT) [8–13], provides quantitative data and higher spatial resolution. Galligas aerosols (prepared with a Technegas generator) are approximately five times smaller than DTPA aerosols [7], leading to less clumping in central airways. Thus, ^{68}Ga PET/CT may improve the performance of V/Q imaging and allow for a better understanding of V/Q matching compared to conventional approaches based on scintigraphy or SPECT. Previous work performed

quantitative pixel- or voxel-wise analysis of V/Q relationships using krypton-81 m (^{81m}Kr)/^{99m}Tc scintigraphy [14], ^{99m}Tc SPECT [15] and ^{68}Ga PET/CT [16] in patients with pulmonary embolism, demonstrating significantly greater V/Q mismatch in patients with embolism than those without. In lung cancer, Le Roux *et al.* [12] used ^{68}Ga PET/CT to evaluate matching of ventilation and perfusion defect or non-defect regions, while quantitative voxel-wise analysis has not been performed.

The purpose of this study was twofold: 1) to quantify V/Q relationships at a voxel level in lung cancer patients using ^{68}Ga PET/CT; and 2) to compare ^{68}Ga PET/CT-measured V/Q matching as a surrogate for gas exchange with diffusing capacity of the lung for carbon monoxide (D_{LCO}), a pulmonary function test (PFT) measurement, as a reference standard.

2. Methods and materials

2.1. Patients

The same 30 consecutive patients with locally advanced or inoperable non-small cell lung cancer (NSCLC) included in the study by Le Roux *et al.* [12] were evaluated for inclusion in this study. All patients underwent ^{68}Ga PET/CT V/Q imaging and PFT and were scheduled to undergo definitive radiotherapy in a clinical trial (Australian-New-Zealand Clinical Trial Registry ID 12613000061730). Patients were excluded from this study if complete 4-dimensional (4D) PET/CT image datasets were not available, substantially low ^{68}Ga signal in the lungs, the entire lungs were not within the field of view, or D_{LCO} was missing. We identified 19 evaluable patients for this study. The median age was 67 years (range 46–89 years). Twelve patients (63%) were male, and seven patients (37%) were female. Tumor stage was as follows: T1 (6 patients, 32%), T2 (4 patients, 21%), T3 (7 patients, 37%) and T4 (2 patients, 11%), and nodal stage was as follows: N0 (7 patients, 37%), N1 (4 patients, 21%), N2 (6 patients, 32%) and N3 (2 patients, 11%). Two patients (11%) had metastatic disease. The study was approved by the institutional ethics committee. All patients provided written informed consent.

2.2. ^{68}Ga PET/CT V/Q imaging

^{68}Ga PET/CT V/Q imaging was performed based on: 1) 4D CT; 2) 4D PET following inhalation of ^{68}Ga-Galligas; and 3) 4D PET following intravenous injection of ^{68}Ga-MAA. Further details have been previously described [11]. The PET images were corrected for attenuation and scatter. The end-expiration phase of 4D PET/CT image datasets, which showed the highest spatial overlap between the PET- and CT-defined lungs [11], were used for the analysis in this study.

2.3. Image processing and analysis

The CT image datasets were resampled to the dimensions of the PET image datasets. The end-expiration phases of 4D PET and CT image datasets were rigidly co-registered. Residual activities from the PET ventilation scan were subtracted after decay correction from the PET perfusion image datasets in a similar manner to Willowson *et al.* [17]. The CT images were segmented to define lung volumes using a region growing method and manual trimming. The PET images were segmented by thresholding with manually selected threshold values that removed major activity spillover out of the CT-defined lung volumes. Only PET voxels within the CT-defined lung volumes were included in the statistical analysis. Within the CT-defined lung volumes, PET voxels with values above and below the same threshold were classified as ventilated (or perfused) and non-ventilated (or non-perfused) voxels, respectively. The PET image value of each voxel was normalized to the total value of all voxels within the CT-defined lung volumes. V/Q ratios were calculated for individual voxels using the normalized PET ventilation and perfusion values in a similar manner to previous studies

showing correlations between V/Q imaging measurements and gas exchange impairment [14,15,18–20]. A base-10 logarithm was applied to produce a symmetric measure for V/Q mismatch. Gas exchange efficiency is maximum when ventilation and perfusion are perfectly matched (V/Q = 1.0, *i.e.*, log(V/Q) = 0), and decreases with increasing deviations of log(V/Q) values from zero due to pathological conditions [3,21]. Fig. S1 in the supplementary materials shows a flowchart of image processing/analysis performed in this study.

2.4. PFT

As part of PFT, D_{LCO} was measured according to the American Thoracic Society and European Respiratory Society guidelines [22]. The percent predicted D_{LCO} was used for the analysis in this study.

2.5. Statistical analysis

V/Q relationships were quantified with voxel-wise Spearman's rank correlations (*r*) between the PET ventilation and perfusion images for each patient. Furthermore, we calculated the percent gas exchanging lung volume, defined as the proportion of voxels that were either ventilated or perfused (determined by thresholding) and had a log(V/Q) value falling within a threshold range to the total number of voxels, and compared with D_{LCO}. Thresholds were set based on a deviation from zero and changed between 0.05 and 0.4 in increments of 0.05. For example, a threshold of 0.4 would include voxels with a log(V/Q) value falling within a range between −0.4 and 0.4. Voxels that were neither ventilated nor perfused were not considered to participate in gas exchange, and hence excluded from the numerator. The correlation between the percent gas exchanging lung volume and the percent predicted D_{LCO} was calculated with the Spearman's rank correlation.

3. Results

Voxel-wise correlations between the PET ventilation and perfusion images varied widely between 19 patients, with *r* ranging from 0.26 to 0.88. Fig. 1 shows PET ventilation and perfusion images and voxel-wise correlations between the two for two representative patients (cases 1 and 19). In case 1, ventilation and perfusion were highly correlated with *r* of 0.88, despite heterogeneous distributions of each of the two. In contrast, ventilation and perfusion were poorly correlated with *r* of 0.26 in case 19.

Fig. 2 shows PET-measured log(V/Q) images and frequency distributions for two representative patients (cases 6 and 11). Case 6 had a larger percent gas exchanging lung volume (91%) determined with a log(V/Q) threshold deviation of 0.25, *i.e.*, 91% of the voxels within the CT-defined lung volumes were either ventilated or perfused and had a log(V/Q) value falling within a range between −0.25 and 0.25. This case showed a homogeneous distribution of log(V/Q) with a nearly normal frequency distribution without major skewness. In contrast, case 11 had a smaller percent gas exchanging lung volume (75%), showing a heterogeneous distribution of log(V/Q) throughout the lungs with a skewed and dispersed frequency distribution. Among the eight different threshold deviations (between 0.05 and 0.4 in increments of 0.05) used to determine the percent gas exchanging lung volume, a threshold deviation of 0.25 demonstrated the highest Spearman's rank correlation (*r* = 0.59, *P*<0.01) between the percent gas exchanging lung volume and D_{LCO} for the 19 patients as shown in Fig. S2 in the supplementary materials. Table S1 in the supplementary materials shows correlations and *P*-values as a function of the threshold deviation.

4. Discussion

To the best of our knowledge, this is the first PET/CT-based quantitative assessment of V/Q relationships at a voxel level in lung cancer patients. This study demonstrated that voxel-wise correlations between
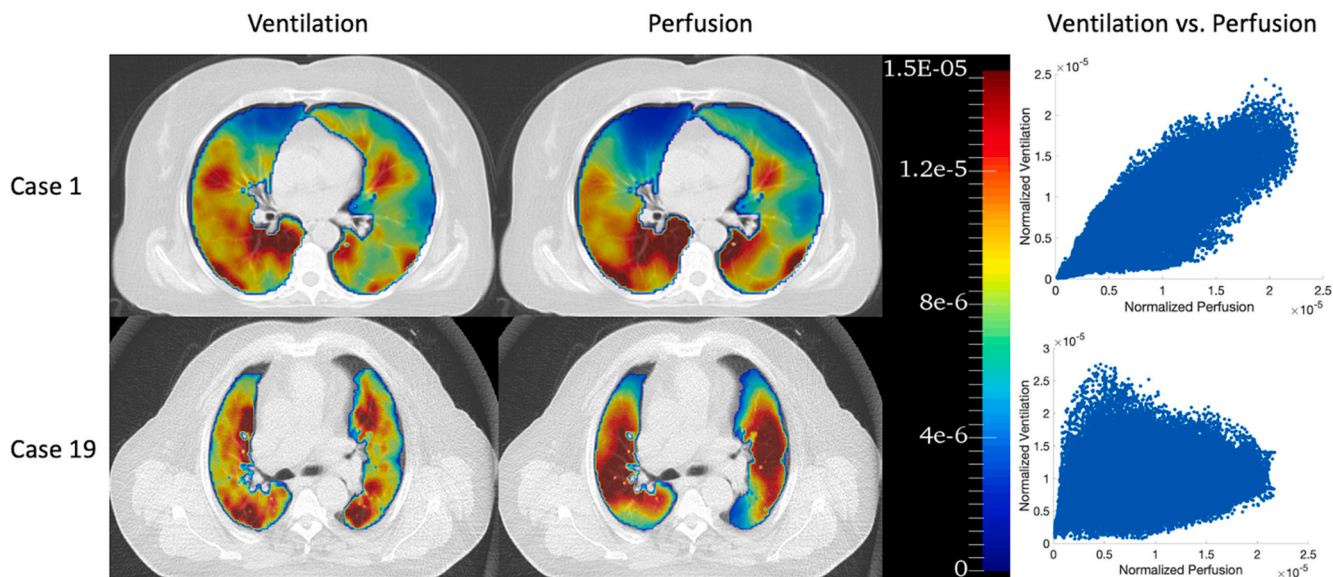
Fig. 1. ^{68}Ga PET/CT ventilation and perfusion images and voxel-wise correlations between ventilation and perfusion for two representative patients: case 1 with the highest correlation ($r = 0.88$) and case 19 with the lowest correlation ($r = 0.26$). Both ventilation and perfusion images are normalized to the total value of all voxels in the CT-defined lung volumes.
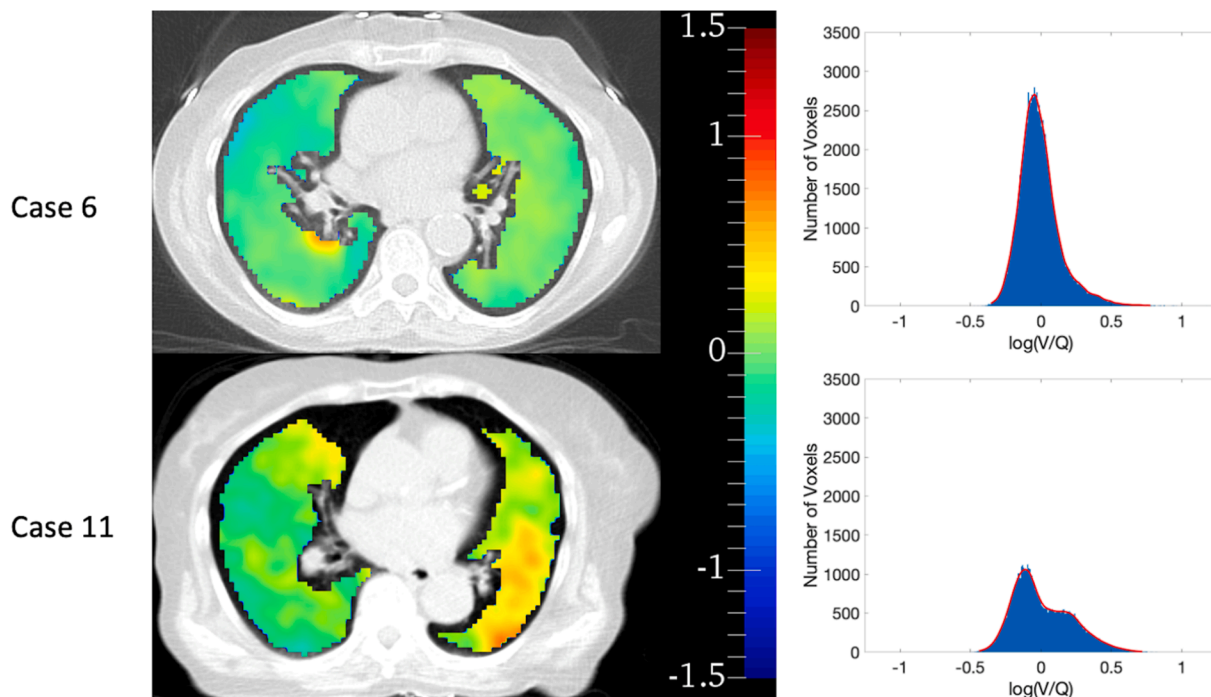

Fig. 2. ^{68}Ga PET/CT-measured log(V/Q) images and frequency distributions for two representative patients: case 6 with a larger percent gas exchanging lung volume (91%) and higher D_{LCO} (81% predicted) and case 11 with a smaller percent gas exchanging lung volume (75%) and lower D_{LCO} (43% predicted). The percent gas exchanging lung volume was determined with a threshold deviation of 0.25. Voxels with no log(V/Q) values in case 11 were neither ventilated nor perfused (determined by thresholding).

ventilation and perfusion varied widely between patients, suggesting that V/Q imaging provides unique and complementary information for physiologic assessment of lung cancer patients.

Our findings are consistent with those of a previous study by Sando *et al.* [4] reporting wide variations in the standard deviation of SPECT-measured V/Q ratio among lung cancer patients. We also demonstrated a significant and moderate correlation between the percent gas exchanging lung volume (defined as the proportion of voxels with V/Q ratios falling within a threshold to the total number of voxels) and D_{LCO},

suggesting that ^{68}Ga PET/CT V/Q imaging may provide a reasonable surrogate for gas exchange. The study by Le Roux *et al.* [12] reported a comparable correlation (0.55) between the percent mismatched defect regions and D_{LCO} based on region-wise (not voxel-wise) analysis.

Imaging of ventilation or perfusion alone has been used in radiotherapy for lung cancer to guide functional avoidance radiotherapy planning and to predict pulmonary toxicity after radiotherapy [1,2]. Given the basic physiologic principle that gas exchange is the primary function of the lungs and previous work demonstrating an association

between D_{LCO} and toxicity [23–26], V/Q imaging may serve as a better imaging biomarker for planning and improve toxicity prediction compared to imaging of ventilation or perfusion alone. Furthermore, V/Q imaging offers opportunities for applications in pulmonary medicine, such as early detection and phenotyping of COPD [27], assessment of severity of infection with severe acute respiratory syndrome coronavirus 2 (SARS-CoV-2) and response to therapy [28].

We acknowledge several limitations to D_{LCO} used as reference to compare with ^{68}Ga PET/CT-measured V/Q matching. First, D_{LCO} only provides global measurements of lung function, and hence are insensitive to local abnormalities. Second, D_{LCO} is influenced by not only local V/Q matching (although regarded as most important [3]) but also structural properties, *e.g.*, thickness of the alveolar-capillary membrane. Comparisons with gas exchange imaging, such as hyperpolarized xenon-129 (^{129}Xe) magnetic resonance imaging (MRI) [29], would provide greater insights into the accuracy of ^{68}Ga PET/CT V/Q imaging as a surrogate for regional gas exchange. However, such studies would be challenging because of limited availability of ^{68}Ga PET/CT as well as ^{129}Xe MRI. Comparisons with ground truth (histopathology) is also challenging. Another limitation of this study is uncertainty in perfusion quantification. The mean ratio of overall ^{68}Ga-MAA activity concentration in the lungs to overall ^{68}Ga-Galligas activity concentration in the lungs was 7.8 (standard deviation, 3.3), which is higher than a ratio of 4 that is generally considered sufficient for perfusion evaluation [30]. However, two cases had a ratio of < 4 (2.2 in case 4 and 3.0 in case 5), which might have influenced perfusion quantification. Although residual activities of ^{68}Ga-Galligas were accounted for by image subtraction, its clearance was not considered and resulting uncertainty in perfusion quantification could be substantial especially if the activity ratio is low.

In conclusion, this study demonstrated that voxel-wise correlations between ^{68}Ga PET/CT-measured ventilation and perfusion varied widely between patients and that the percent gas exchanging lung volume was correlated significantly and moderately with D_{LCO}. Our findings suggested that ^{68}Ga PET/CT V/Q imaging could provide unique and complementary information and a reasonable surrogate for regional gas exchange for physiologic assessment of lung cancer patients.

Declaration of Competing Interest

The authors declare that they have no known competing financial interests or personal relationships that could have appeared to influence the work reported in this paper.

Acknowledgements

Appendix A. Supplementary data

Supplementary data to this article can be found online at https://doi.org/10.1016/j.phro.2022.03.005.

References

[1] Bucknell NW, Hardcastle N, Bressel M, Hofman MS, Kron T, Ball D, et al. Functional lung imaging in radiation therapy for lung cancer: A systematic review and meta-analysis. Radiother Oncol 2018;129:196–208. https://doi.org/10.1016/j.radonc.2018.07.014.

[2] Faught AM, Miyasaka Y, Kadoya N, Castillo R, Castillo E, Vinogradskiy Y, et al. Evaluating the Toxicity Reduction With Computed Tomographic Ventilation Functional Avoidance Radiation Therapy. Int J Radiat Oncol Biol Phys 2017;99:325–33. https://doi.org/10.1016/j.ijrobp.2017.04.024.

[3] Glenny RW, Robertson HT. Spatial distribution of ventilation and perfusion: mechanisms and regulation. Compr Physiol 2011;1:373–95.

[4] Sando Y, Inoue T, Nagai R, Endo K. Ventilation/perfusion ratios and simultaneous dual-radionuclide single-photon emission tomography with krypton-81m and technetium-99m macroaggregated albumin. Eur J Nucl Med 1997;24:1237–44.

[5] Suga K, Kawakami Y, Zaki M, Yamashita T, Shimizu K, Matsunaga N. Clinical utility of co-registered respiratory-gated(99m)Tc-Technegas/MAA SPECT-CT images in the assessment of regional lung functional impairment in patients with lung cancer. Eur J Nucl Med Mol Imaging 2004;31:1280–90. https://doi.org/10.1007/s00259-004-1558-1.

[6] Yuan ST, Frey KA, Gross MD, Hayman JA, Arenberg D, Curtis JL, et al. Semiquantification and classification of local pulmonary function by V/Q single photon emission computed tomography in patients with non-small cell lung cancer: potential indication for radiotherapy planning. J Thorac Oncol 2011;6:71–8. https://doi.org/10.1097/JTO.0b013e3181f77b40.

[7] Petersson J, Sanchez-Crespo A, Larsson SA, Mure M. Physiological imaging of the lung: single-photon-emission computed tomography (SPECT). J Appl Physiol 2007;102:468–76. https://doi.org/10.1152/japplphysiol.00732.2006.

[8] Mathias CJ, Green MA. A convenient route to [68Ga]Ga-MAA for use as a particulate PET perfusion tracer. Appl Radiat Isot 2008;66:1910–2. https://doi.org/10.1016/j.apradiso.2008.06.004.

[9] Kotzerke J, Andreeff M, Wunderlich G. PET aerosol lung scintigraphy using Galligas. Eur J Nucl Med Mol Imaging 2010;37:175–7. https://doi.org/10.1007/s00259-009-1304-9.

[10] Hofman MS, Beauregard JM, Barber TW, Neels OC, Eu P, Hicks RJ. 68Ga PET/CT ventilation-perfusion imaging for pulmonary embolism: a pilot study with comparison to conventional scintigraphy. J Nucl Med 2011;52:1513–9. https://doi.org/10.2967/jnumed.111.093344.

[11] Callahan J, Hofman MS, Siva S, Kron T, Schneider ME, Binns D, et al. High-resolution imaging of pulmonary ventilation and perfusion with 68Ga-VQ respiratory gated (4-D) PET/CT. Eur J Nucl Med Mol Imaging 2014;41:343–9. https://doi.org/10.1007/s00259-013-2607-4.

[12] Le Roux PY, Siva S, Steinfort DP, Callahan J, Eu P, Irving LB, et al. Correlation of 68Ga Ventilation-Perfusion PET/CT with Pulmonary Function Test Indices for Assessing Lung Function. J Nucl Med 2015;56:1718–23. https://doi.org/10.2967/jnumed.115.162586.

[13] Le Roux PY, Hicks RJ, Siva S, Hofman MS. PET/CT Lung Ventilation and Perfusion Scanning using Galligas and Gallium-68-MAA. Semin Nucl Med 2019;49:71–81. https://doi.org/10.1053/j.semnuclmed.2018.10.013.

[14] Itti E, Nguyen S, Robin F, Desarnaud S, Rosso J, Harf A, et al. Distribution of ventilation/perfusion ratios in pulmonary embolism: an adjunct to the interpretation of ventilation/perfusion lung scans. J Nucl Med 2002;43:1596–602.

[15] Harris B, Bailey D, Miles S, Bailey E, Rogers K, Roach P, et al. Objective analysis of tomographic ventilation-perfusion scintigraphy in pulmonary embolism. Am J Respir Crit Care Med 2007;175:1173–80. https://doi.org/10.1164/rccm.200608-1110OC.

[16] Oehme L, Zophel K, Golgor E, Andreeff M, Wunderlich G, Brogsitter C, et al. Quantitative analysis of regional lung ventilation and perfusion PET with (68)Ga-labelled tracers. Nucl Med Commun 2014;35:501–10. https://doi.org/10.1097/MNM.0000000000000084.

[17] Willowson K, Bailey DL, Baldock C. Quantitative SPECT reconstruction using CT-derived corrections. Phys Med Biol 2008;53:3099–112. https://doi.org/10.1088/0031-9155/53/12/002.

[18] Vidal Melo MF, Winkler T, Harris RS, Musch G, Greene RE, Venegas JG. Spatial heterogeneity of lung perfusion assessed with (13)N PET as a vascular biomarker in chronic obstructive pulmonary disease. J Nucl Med 2010;51:57–65. https://doi.org/10.2967/jnumed.109.065185.

[19] Jobse BN, Rhem RG, Wang IQ, Counter WB, Stampfli MR, Labiris NR. Detection of lung dysfunction using ventilation and perfusion SPECT in a mouse model of chronic cigarette smoke exposure. J Nucl Med 2013;54:616–23. https://doi.org/10.2967/jnumed.112.111419.

[20] Hwang HJ, Seo JB, Lee SM, Kim N, Oh SY, Lee JS, et al. Assessment of Regional Xenon Ventilation, Perfusion, and Ventilation-Perfusion Mismatch Using Dual-Energy Computed Tomography in Chronic Obstructive Pulmonary Disease Patients. Invest Radiol 2016;51:306–15. https://doi.org/10.1097/RLI.0000000000000239.

[21] Petersson J, Glenny RW. Gas exchange and ventilation-perfusion relationships in the lung. Eur Respir J 2014;44:1023–41. https://doi.org/10.1183/09031936.00037014.

[22] Macintyre N, Crapo RO, Viegi G, Johnson DC, van der Grinten CP, Brusasco V, et al. Standardisation of the single-breath determination of carbon monoxide uptake in the lung. Eur Respir J 2005;26:720–35. https://doi.org/10.1183/09031936.05.00034905.

[23] Abratt RP, Willcox PA, Smith JA. Lung cancer in patients with borderline lung functions–zonal lung perfusion scans at presentation and lung function after high dose irradiation. Radiother Oncol 1990;19:317–22.

[24] Marks LB, Munley MT, Bentel GC, Zhou SM, Hollis D, Scarfone C, et al. Physical and biological predictors of changes in whole-lung function following thoracic irradiation. Int J Radiat Oncol Biol Phys 1997;39:563–70 [pii] https://doi.org/S0360-3016(97)00343-X.

[25] Videtic GM, Stitt LW, Ash RB, Truong PT, Dar AR, Yu EW, et al. Impaired diffusion capacity predicts for decreased treatment tolerance and survival in limited stage small cell lung cancer patients treated with concurrent chemoradiation. Lung Cancer 2004;43:159–66.

[26] Lopez Guerra JL, Gomez D, Zhuang Y, Levy LB, Eapen G, Liu H, et al. Change in diffusing capacity after radiation as an objective measure for grading radiation

pneumonitis in patients treated for non-small-cell lung cancer. Int J Radiat Oncol Biol Phys 2012;83:1573–9. https://doi.org/10.1016/j.ijrobp.2011.10.065.

[27] Gefter WB, Lee KS, Schiebler ML, Parraga G, Seo JB, Ohno Y, et al. Pulmonary Functional Imaging: Part 2-State-of-the-Art Clinical Applications and Opportunities for Improved Patient Care. Radiology 2021;299:524–38. https://doi.org/10.1148/radiol.2021204033.

[28] Tipre DN, Cidon M, Moats RA. Imaging Pulmonary Blood Vessels and Ventilation-Perfusion Mismatch in COVID-19. Mol Imaging Biol 2022. https://doi.org/10.1007/s11307-021-01700-2.

[29] Driehuys B, Cofer GP, Pollaro J, Mackel JB, Hedlund LW, Johnson GA. Imaging alveolar-capillary gas transfer using hyperpolarized 129Xe MRI. Proc Natl Acad Sci U S A 2006;103:18278–83. https://doi.org/10.1073/pnas.0608458103.

[30] Palmer J, Bitzen U, Jonson B, Bajc M. Comprehensive ventilation/perfusion SPECT. J Nucl Med 2001;42:1288–94.